

## Three Dimensional Graphene Oxide-Carbon Nanotubes and Graphene-Carbon Nanotubes Hybrids

Veerappan Mani<sup>1</sup>, Shen-Ming Chen<sup>1\*</sup>, Bih-Show Lou<sup>2,\*</sup>

<sup>1</sup>Electroanalysis and Bioelectrochemistry Lab, Department of Chemical Engineering and Biotechnology, National Taipei University of Technology, Taipei 106, Taiwan

<sup>2</sup>Chemistry Division, Center for General Education, Chang Gung University, Tao-Yuan, Taiwan.

\*E-mail: [smchen78@ms15.hinet.net](mailto:smchen78@ms15.hinet.net)(Shen-Ming Chen); [blou@mail.cgu.edu.tw](mailto:blou@mail.cgu.edu.tw) (Bih-Show Lou)

*Received:* 19 April 2013 / *Accepted:* 5 August 2013 / *Published:* 1 September 2013

---

Graphene and carbon nanotubes (CNT) are two important nanomaterials having exceptional physicochemical properties, revolutionized the entire research world and enjoyed widespread applications. Recently several efforts were made to assemble these two nanomaterials to prepare 3D hierarchical graphene-CNT hybrid with synergic properties of CNTs and graphene. The combination of 2D graphene of high charge density and 1D CNTs of large surface area generates a versatile 3D graphene-CNT hybrid network with synergic properties. Herein, we review the recent progress in the various preparation methodologies of graphene oxide (GO) -CNT and graphene-CNT hybrid nanomaterials (GO/graphene-CNT) and their characterization studies. In addition, we discussed the outstanding applications of the hybrid material in diverse fields of research including supercapacitors, dye sensitized solar cells (DSSCs), sensors, biosensors and batteries.

---

**Keywords:** graphene, graphene oxide, GO/graphene-CNT, CNT, hybrid materials, electrochemistry, electrochemical, preparation, characterization and applications.

### 1. INTRODUCTION

Graphene, a two dimensionally arranged and densely packed honeycomb lattice with  $sp^2$  hybridized carbon atoms is the thinnest known material in the universe till date [1-3]. Graphene is one of the special allotrope of carbon, become ‘rising star’ among all other carbon nanomaterials in various fields of research owing to its unique physicochemical properties [4-6]. Its unique properties include high surface area, tunable band gap, room temperature Hall effect, excellent electrical, thermal and conducting properties [7-8]. It can be viewed as mother of other graphitic allotrope forms; it can wrap into fullerene (0D), rolled up into carbon nanotubes (1D) and stacked into multilayered graphite (3D)

[9, 10]. It shows great potential applications in various fields of research such as electronics [11], photocatalysis [12], solar cells [13], supercapacitors [14], medicine [15] sensors [16] and biosensors [17].

Graphene can be prepared by number of methods such as micromechanical exfoliation, Epitaxial growth on silicon carbide, chemical vapor deposition (CVD), Arc discharge method, small molecules intercalation within multilayered graphite, unzipping of CNTs, electrochemical method and chemical reduction of exfoliated GO [10, 18]. Each method holds its own advantages and disadvantages. Mechanical exfoliation of highly oriented pyrolytic graphite, also called as simple scotch tape method offer high quality graphene for the electronic applications with the associated disadvantages of low yield of graphene [1]. CVD growth of hydrocarbons on transition metal substrates (Cu, Ni, Co) [19, 20-34] and epitaxial growth of graphene layers on silicon carbide can provide bulk quantity of graphene, but requires high temperature and high cost [21, 22]. Intercalation of small molecules and subsequent exfoliation (via thermal shock [23], microwave exfoliation [24], sonication approaches [25]) eventually break the multilayered graphite network into monolayered graphene sheets with high quality and defects free [26]. Numbers of approaches were made to prepare high quality graphene sheets via unzipping of CNTs which has the disadvantage of time consuming process [27, 28]. Chemical methods involve use of cheap and easily available graphite powder as the starting precursor with the simple set of process involving oxidation, exfoliation and reduction respectively [29].

Chemical oxidation of graphite to graphite oxide, its exfoliation to monolayered graphene oxide (GO) and its subsequent reduction to graphene is one of the efficient approach to prepare scalable bulk quantity of graphene [30]. Chemical oxidation of graphite can be achieved by Brodie method [31], Staudenmaier method [32] and Hummer's method [33, 34]. Exfoliation of graphite oxide can be achieved by microwave assistance [35], ultrasonication [36] and thermally [37]. Reduction of GO can be performed by using reducing agents (hydrazine [16], sodium borohydride [38], hydroquinone [39], ascorbic acid [40], alcohols [41], alkali solutions [42, 43], and reducing sugars [44] such as glucose, fructose and sucrose) thermal methods [45], and electrochemical reduction methods [46, 47]. Though the chemical oxidation-reduction approach give low quality graphene with residual oxygen functionalities and structural defects, until now this is the most versatile and desirable route for the production of bulk quantities of graphene for many applications [48]. Specifically, chemical oxidation-reduction method has profound impact for the electrochemical applications where the defects and residual functional groups have specific advantage. The ambitious vision to find a perfect method for the synthesis of defect free, bulk quantity of high quality graphene with 100%  $sp^2$  carbon atoms of perfect planar structure is a long time goal in the field of graphene based research.

Graphene oxide (GO), oxygenated derivative of graphene is an amphiphilic molecule having the structural network of interconnected random distribution of aliphatic and aromatic regions [49]. GO possess hydrophilicity owing to the presence of oxidized aliphatic regions containing tetrahedral  $sp^3$  carbon atoms, whereas hydrophobicity is due to the presence of aromatic regions with unoxidised benzene rings containing planar  $sp^2$  carbon atoms [50]. It contains numerous functional groups mainly epoxy and hydroxyl groups on the plane, whereas carboxyl, carbonyl, ester, ether, diol, ketone, phenol, quinine and lactones groups present at the edge surfaces of the GO sheets [51, 52]. The oxygen

functionalities present on the basal and edge planes render it for the high dispersion in aqueous solutions and pave a way for the chemical functionalization [49], such as amidation at the carboxylic groups [53] and nucleophilic substitution via epoxy groups [54]. On the other hand, the aromatic regions having  $sp^2$  networks provide active sites to interact with other aromatic molecules through  $\pi$ - $\pi$  supramolecular interactions [55]. Thus GO is a very important precursor compound for the preparation of graphene based composite materials with metals, metal oxides, polymers and CNTs for the diverse range of applications.

Carbon nanotubes (CNTs), viewed as rolled version of graphene sheets is another well known allotrope of carbon owns unique electrical, mechanical, catalytic and electrocatalytic properties and dominated the entire material science research since its discovery in 1991 [56]. In the past two decades, enormous amount of works have been done on both multiwalled carbon nanotubes (MWCNT) and single walled carbon nanotubes (SWCNTs) [57-61]. Generally CNTs tend to agglomerate in organic dispersion; therefore numerous efforts were developed to disperse the CNT by using micelles, ionic liquids, surfactants, polymer wrapping and other chemical functionalization approaches [62-63]. It has been proved that GO could be a better dispersant to form a stable dispersion of CNT and the resulted dispersion is a novel hybrid named as graphene oxide-CNT (GO-CNT) [64]. Studies proved that GO-CNT and graphene-CNT hybrid nanomaterials exhibit higher electrical conductivities, large specific area and catalytic properties compared with either pristine CNTs or GO/graphene [64-66]. The hybrids were prepared by several approaches including simple sonication method [64, 66], CVD method [67] and electrostatic spray technique [68]. The strong  $\pi$ - $\pi$  stacking interaction operating between graphene and CNT make a 3D network for the hybrid material and provide exceptional stability [69].

Stoner et al. [70] presented detailed studies on the classification of carbon nanostructures based on dimensional organization of their edge structures and they found that the 3D hierarchical arrangement of the graphene-CNT hybrid possess both the high charge density of graphene and 3D network of CNT with large surface area. As a result it have the outstanding characteristics with highest edge density per unit nominal area than the other carbon nanostructures (graphite, MWCNT, SWCNT, graphene sheets, activated carbon, aligned CNT, HOPG and bamboo CNT) make it as the best candidate owning outstanding properties among all other carbon nanostructures counterparts. Most of the reports claimed that the synergic effect operating between graphene and CNT is responsible for the improved capacitance of the graphene-CNT hybrid. On the contrary, Pumera and co-workers [71] showed that the improved capacitance of the hybrid is because of arithmetic average of weight specific capacitances of graphene and CNTs and there is no any synergic effect operating between them.

Eventhough graphene-CNT composite (some authors referred it as reduced graphene oxide-CNT or RGO-CNT) was prepared recently, its outstanding properties and ease of preparation methods find a way for the applications in all the fields of research. Herein, we review the various preparation methodologies, characterization and applications of the both CNTs-graphene (or reduced graphene oxide, RGO) and GO-CNT hybrid materials in various fields of research include supercapacitors, solar cells, sensors, biosensor and fuel cells. For the sake of convenience, GO-CNT and graphene-CNT hybrid materials together refereed as GO/graphene-CNT hybrid in this entire manuscript.

## 2. PREPARATION STRATEGIES FOR GO/GRAPHENE-CNT HYBRID MATERIAL.

### 2.1 GO-CNT hybrid

One of the most widely used approach for the preparation of GO-CNT hybrid is simply mixing GO and CNT in appropriate ratios and followed by ultrasonic treatment [64, 69, 72-81]. For instance, Tian et al. [72] prepared optically transparent solution-like aqueous suspensions of GO-SWCNT hybrid by simply dispersing the purified SWCNTs into GO and subsequent treatment of ultrasonication. The authors found that the optimum weight ratio between GO and SWCNTs was  $\geq 1$  to get stable hybrid. Moreover they demonstrated the application of hybrid material towards accurate determination of absorptivities in the band-gap transitions.

Zheng and co-workers [82] prepared large-area hybrid transparent films of GO-SWCNT hybrid by layer-by-layer Langmuir–Blodgett (L–B) assembly process without using any intermediate transfer process. The conductivity of the prepared GO-SWCNT thin films is  $\approx 400 \Omega \text{ sq}^{-1}$  at 84% transmittance, showed the efficiency of this preparation approach. Efforts were made to improve the quality of the GO-MWCNT hybrid by including electrostatic spray technique after the treatment of ultrasonication [68]. Kim et al. [83] synthesized scrolled GO-MWCNT hybrid material via covalent bond linkage.

Zhang and co-workers [69] prepared the GO-MWCNT composite material by simple sonication of GO and MWCNT. The preparation steps consisting (1) preparation of graphite oxide by Hummers method, (2) exfoliation of graphite oxide to GO, (3) mixing CNT and GO solution in a fixed ratio, (4) Ultrasonication of the mixture and (5) removal of loosely bounded MWCNT and excess GO by subjecting two centrifugation cycles (30 min each) at 8000 and 14000 RPM, respectively.

Therefore, most of the methods presented for the preparation of GO-CNT hybrid were of very simple procedures and green not involving use of any hazardous chemicals or any difficult experimental conditions.

### 2.2 Preparation of graphene-CNT hybrid material

#### 2.2.1 Solution based approaches: Simple sonication and reduction

Among other methods available for the preparation of graphene-CNT hybrid, two simple methods were used often, (1) preparation of GO-CNT hybrid by ultrasonication of GO and CNT mixture (2) subsequent reduction of GO-CNT hybrid to graphene with some specific post treatments [84-92]. As mentioned in the case of pristine graphene oxide reduction, the reduction of incorporated GO in GO-CNT hybrid can also be performed by various methods including chemical [86], thermal, electrochemical [50], photochemical and hydrothermal [87] methods.

Zhang et al. [88] prepared graphene-CNT hybrid composite by ultrasonication of GO and MWNCT mixture and followed by thermal reduction of the resulting GO-MWCNT composite. Yen and coworkers [66] reported a two-step solution-based method at room temperature for the preparation of graphene–MWCNT hybrid material comprising graphene and acid-treated MWCNT (Fig. 1). Briefly, the preparation methods involves, (1) synthesis of graphene oxide from graphite by Staudenmaier's method and consequent thermal reduction to graphene at 1050°C. (2) Mixing of

graphene with acid treated MWCNTs and ultrasonication to get the final hybrid. A non-covalent  $\pi$ - $\pi$  stacking interaction operating between graphene sheets and CNTs were revealed, which help to avoid the aggregation of individual graphene sheets.

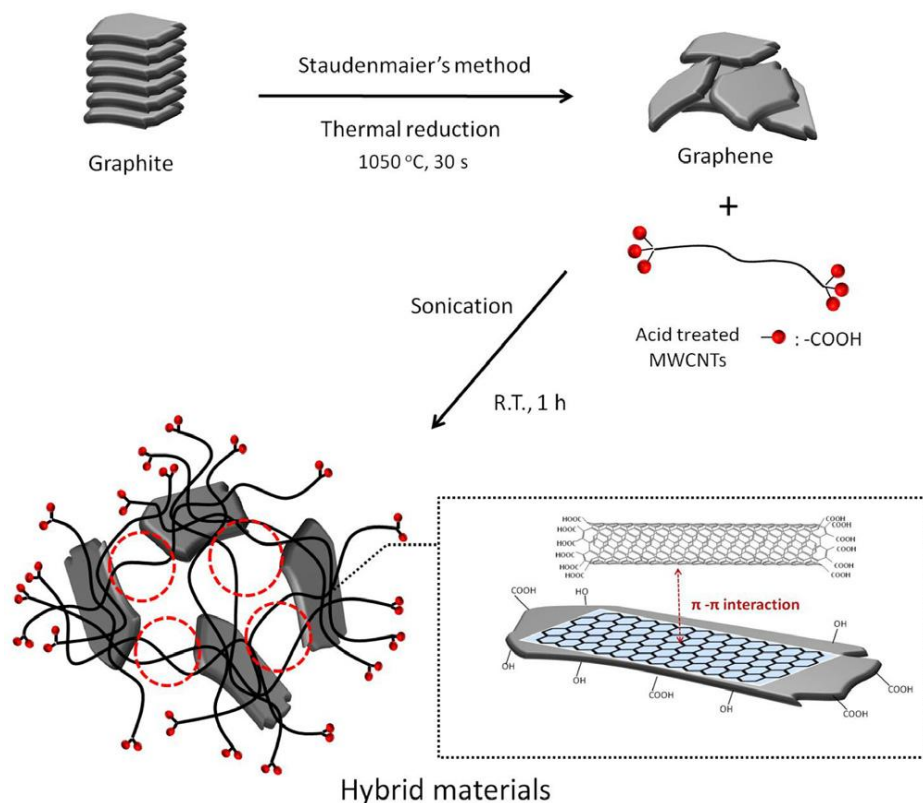


**Figure 1.** The schematic mechanism for the preparation of graphene-CNT hybrid material (Reproduced with permission from ref. [66]).

Sui and co-workers [91] reported a green method for the fabrication of CNT-graphene hybrid aerogels by supercritical  $\text{CO}_2$  drying of the hybrid hydrogel precursors attained by heating the mixtures of GO and CNTs with the aid of Vitamin C. The graphene-CNT aerogels encompass light weight, high conductivity, large BET surface area, and large volume with hierarchically porous structure. Liu et al. [92] prepared the hybrid nanofiller system consisting  $\text{Cu}^{2+}$  coordinated graphene-MWCNT network by solution mixing. The graphene sheets were separated and bridged by nanotubes networks via coordination of  $\text{Cu}^{2+}$  ions and the resulting  $\text{Cu}^{2+}$ -coordinated graphene-MWCNT network can be easily introduced to a range of polymer matrices by simple solution mixing.

It was revealed that electrochemical reduction of GO to graphene was appreciably improved after the incorporation of CNT in comparison with the electrochemical reduction of pristine GO [50, 64]. During the electrochemical reduction by cyclic voltammogram, the onset potential of the cathodic peak appeared for the GO-CNT hybrid (-0.3 V) is much lower than that of pristine GO (-0.7 V). The plausible reason for the significant improvement in the electrochemical reduction of GO in the hybrid was due to the incorporated CNT which bridges the graphene sheets and acts as a conducting wire between graphene sheets.

### 2.2.2 Chemical Vapour Deposition method (CVD)

Numerous efforts were made to prepare graphene-CNT or RGO-CNT by chemical vapour deposition method [67, 93-99]. CVD method of preparation often provide uniformly grown CNTs onto the surface of the graphene sheets via strong interactions, which ultimately avoids restacking of graphene sheets and provide high stability to the hybrid material. Chen and co-workers [94] reported in situ growth of multilayered graphene-CNT composite by CVD process. The chemical vapor reduction and deposition reactions were carried out at 500°C for varied times (2, 5 and 1 h) to obtain various lengths of CNTs on GO sheets. The best performance achieved in the case of graphene-CNT with shortest length grown at 2 min. Therefore, the key factor to prepare a graphene-CNT hybrid of better electrochemical process is tuning the time duration of the CVD process which makes possible to grow CNTs of different lengths.

As well, 3D graphene-CNT sandwich structures consisting CNT pillars grown in between the graphene layers has been prepared by CVD method [99]. (1) GO and CNTs were prepared by modified hummers method and thermal reduction respectively and mixed together in the solution form with the mass ratio of 1:10, (2) subjected to ultrasonication, filtrated and desiccated, (3) CVD process in horizontal quartz tubular reactor at 750°C for 1 h in Ar atmosphere with a flow rate of 300 sccm. The authors make use the obtained graphene-CNT hybrid for the supercapacitors applications and achieved good performance with the maximum specific capacitance value of 385 F g<sup>-1</sup>. Lee et al. [100] reported plasma-enhanced CVD approach for the preparation of graphene-CNT. The process includes (1) Thermal reduction of GO onto silicon wafer (2) Deposition of nanopatterned Fe catalyst onto the GO film using self-assembled block-copolymer templates. (3) Growth of vertical CNTs by plasma-enhanced CVD growth at 600°C. During the PE-CVD process, simultaneously the underlying GO sheets were thermally reduced.

### 2.2.3 Preparation by Self assembly

Some efforts were made to prepare graphene-CNT hybrid film prepared self assembly processes involving simple steps [101-103]. Huang et al. [101] prepared graphene-CNT hybrid by self assembly on a Ti substrate by simple casting method, the process involving, (1) preparation of GO and MWCNTs by modified Hummers method and CVD process respectively, (2) mixing of GO and MWCNT and following ultrasonication to acquire GO-CNT hybrid, (3) self assembly on a Ti sheet to get the hybrid. Li and co-workers [102] proposed vacuum-assisted self-assembly to prepare RGO-MWCNT hybrid sandwich from a dispersion of GO and MWCNTs followed by thermal reduction at 200 °C.

## 3. CHARACTERIZATIONS

A number of techniques have been utilized for the characterization of GO/graphene-CNT hybrid materials, involving scanning electron microscopy (SEM), transmission electron microscopy

(TEM), atomic force microscopy (AFM), X-ray diffraction (XRD), X-ray photoelectron spectroscopy (XPS), cyclic voltammetry (CV), UV-Vis, Raman, and FT-IR spectroscopies [64, 69, 85-89]. These techniques were employed to know the surface morphology, interactions between sheets and tubes, chemical components and electronic properties of the hybrids.

### 3.1 Characterization of GO-CNT hybrid

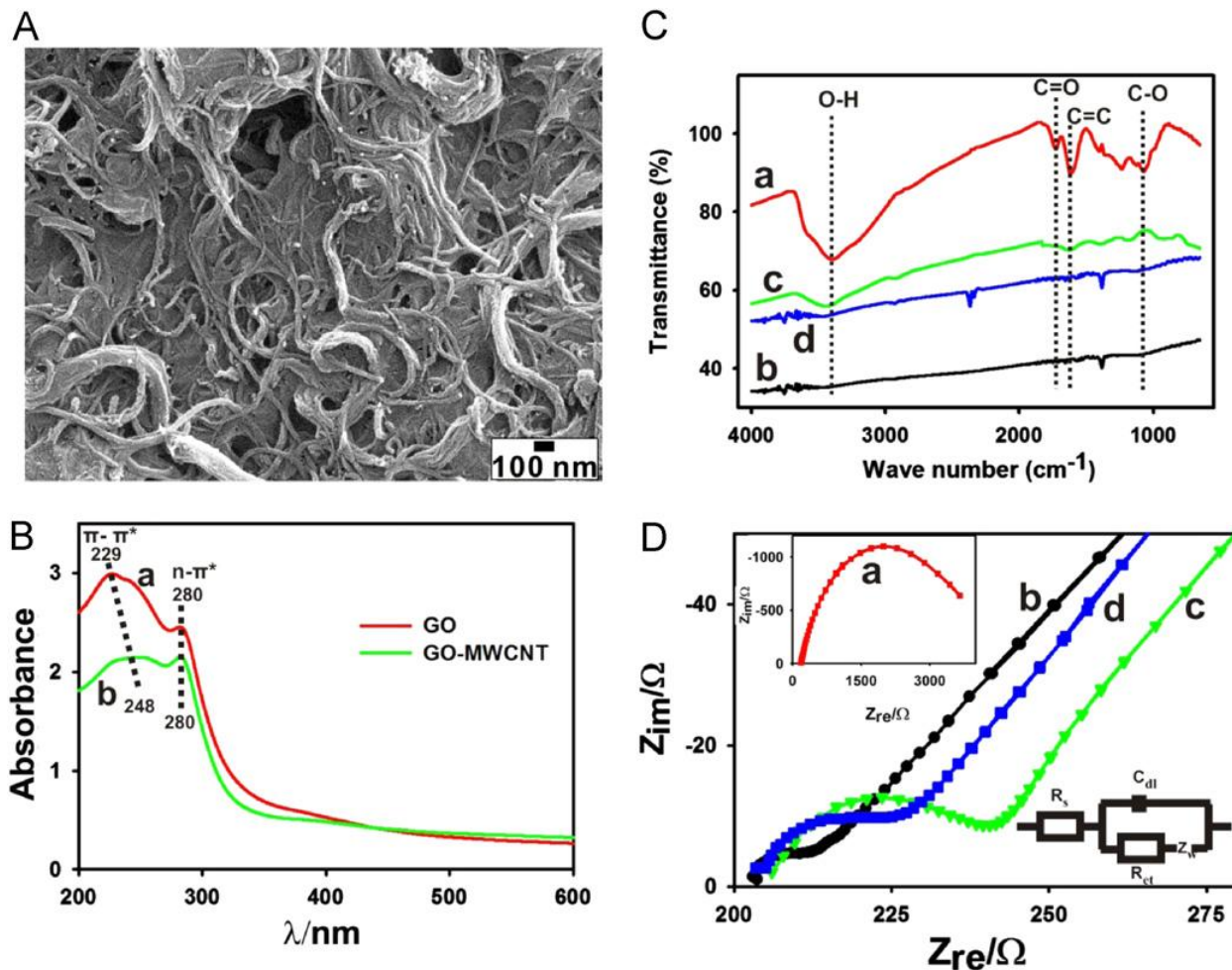


**Figure 2.** (A) FESEM image of GO-MWCNT. (B) UV-Vis absorption spectra of GO (a) and GO-MWCNT hybrid (b). (C) FT-IR spectra and (D) EIS of GO (a), MWCNT (b), GO-MWCNT (c) and RGO-MWCNT (d). (Reproduced with permission from ref. [64])

We prepared the GO-MWCNT composite and characterized by several techniques such as SEM, UV-Vis absorption spectra, FT-IR spectroscopy and electrochemical impedance spectroscopy (EIS) (Fig. 2). The FESEM image of the GO-MWCNT revealed that GO sheets were entirely wrapped by the tubular networks of CNTs via non covalent  $\pi$ - $\pi$  stacking interaction. In addition UV-Vis spectra also performed to confirm the involvement of non covalent  $\pi$ - $\pi$  stacking interaction between the hydrophobic  $sp^2$  hybridized hydrophobic regions of GO and the sidewalls of MWCNT. The bathochromic shift of the  $\pi$  -  $\pi^*$  transition of GO after its incorporation with CNT as GO-CNT hybrid

revealed that the interaction is via  $\pi$ - $\pi$  stacking interaction. FT-IR and EIS results also confirmed the formation of the GO-MWCNT.

### 3.2 Characterisation of graphene-CNT hybrid

Similarly, graphene-CNT hybrid material has been characterised by various available techniques to know the morphology and the bonding interaction involved between CNTs and graphene. For instance, Sasikaladevi and co-workers prepared the graphene-CNT hybrid by CVD method and characterised by various techniques [104]. The surface morphological studies of the hybrid by FESEM and TEM techniques revealed that wrinkled graphene sheets were coated onto the surfaces of CNTs.

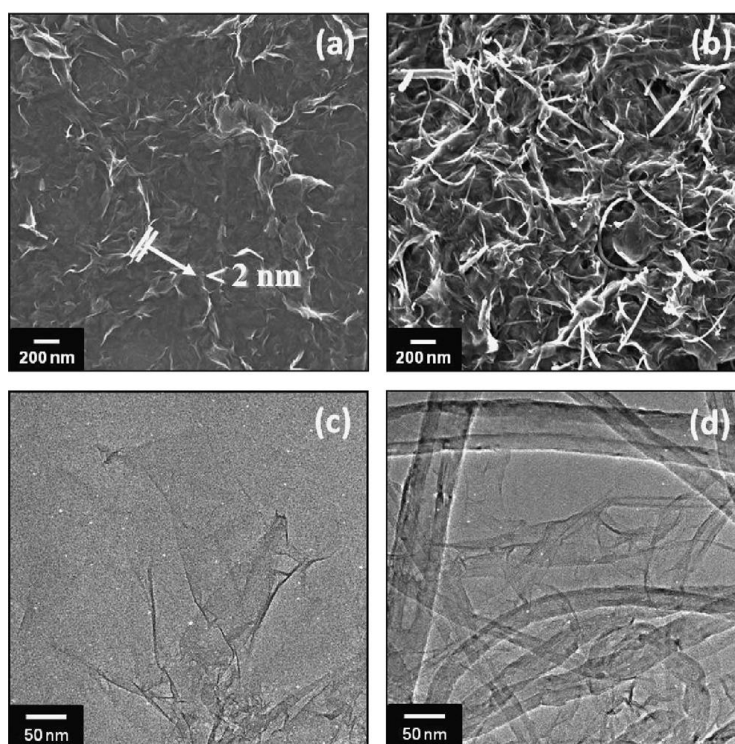


**Figure 3.** SEM of graphene (a) and graphene-MWCNT hybrid (b). HR-TEM of graphene (c) and graphene-MWCNT hybrid (d) (Reproduced with permission from ref. [105]).

The XRD pattern of the graphene-CNT hybrid exhibited two peaks at  $26.42^\circ$  and  $26.49^\circ$  with interlayer spacing of 0.33 and 0.34 nm respectively and the absence of peak at  $10.6^\circ$  (responsible for the oxygen functionalities) confirmed the efficient reduction of GO. From the Raman spectrum, the positions of the bands and ratio of the intensities of the two important bands D and G bands were monitored to follow the structural changes and stacking behaviors during the course of hybrid formation from graphene and CNT [104].

Likewise, Woo and co-workers characterized the graphene-CNT hybrid by various techniques [105]. FESEM and HR-TEM images revealed that the graphene sheets consists of randomly aggregated, thin, crumpled and folded sheets with thickness of 2 nm (Fig. 3). Whereas, the FESEM

image of the graphene–MWCNT hybrid, encompassed homogeneous 3D network of graphene-CNT hybrid with ultrathin graphene sheets placed between CNTs through  $\pi$ - $\pi$  stacking interaction. Likewise HR-TEM images also revealed that MWCNTs networks were fully covered by the graphene sheets. The bonding between MWCNTs and graphene sheets was strong enough to make the graphene sheets adhered well with MWCNT bundles and eventually it avoids the aggregation of graphene sheets and provides high stability for the hybrid. Moreover the authors studied the electrochemical behavior of the hybrid by cyclic voltammogram experiments towards the common redox probe  $\text{Fe}(\text{CN})_6^{3-/4-}$  and found that the electrochemical behavior was greatly enhanced compared with pristine graphene and CNTs. The CNTs were acting as conducting wires between the graphene sheets which resulting in the significant promotion of the conductivity of the hybrid material.

#### 4. GO-CNT HYBRID -APPLICATIONS

GO-CNT hybrid material has been utilized for the various applications including supercapacitors [73, 78, 98], batteries [68], solar cells [106, 107] sensors [79-81, 108] and biosensors [74].

##### 4.1 Supercapacitors

Aboutalebi and co-workers prepared the GO-CNT hybrid composite for the possible application as supercapacitors materials in energy storage devices. The hybrid material showed good synergistic effect leading to higher capacitance compared with either GO or MWCNTs alone. The authors found that the hybrid material exhibited higher capacitance compared to either GO or MWCNTs. A maximum specific capacitances of  $251 \text{ F g}^{-1}$  was achieved at  $5 \text{ mVs}^{-1}$  and a total increase of 120.5% was recorded in 1000 cycles for the hybrid material, which is significantly higher than the specific capacitance achieved for pristine CNT ( $85 \text{ F g}^{-1}$ ) or pristine GO ( $60 \text{ Fg}^{-1}$ ).

##### 4.2 Batteries

Han et al. prepared GO-MWCNT hybrid by electrostatic spray method which exhibited good electrocatalytic redox reversibility towards  $\text{VO}^{2+}/\text{VO}^{2+}$  redox couples for vanadium redox flow batteries. The prepared hybrid showed significantly enhanced electrochemical performance and the  $I_{\text{pa}}/I_{\text{pc}}$  value remains constant at about 1.20, even at higher scan rate. Additionally, the charge transfer resistance across the electrode/electrolyte interface is significantly reduced, especially for the reduction from  $\text{VO}^{2+}$  to  $\text{VO}^{2+}$ . Compared with pristine GO or MWCNT, GO-MWCNTs delivered a much better electrocatalytic redox reversibility towards the positive  $\text{VO}^{2+}/\text{VO}^{2+}$  couple. The excellent performance of the hybrid material proved that the hybrid material grasps great potential for the more development in vanadium redox flow batteries.

### 4.3 Solar cells

GO-SWCNT composite modified thin films were fabricated for the application as an efficient anode modifier for polymer Solar cells [106]. The hybrid offered better performance compared with the conventional PEDOT:PSS anode modifier. The incorporation of SWCNT into GO sheets helped to promote the hole extraction and charge flow in the anode modifying layer and offered higher optical transmission in the longer wavelength regions. Therefore, it is expected that the hybrid material could be an attractive new material as an anode modifier for the development of new low band gap polymer solar cells and possibly the interconnect layer in tandem devices.

### 4.4 Sensors

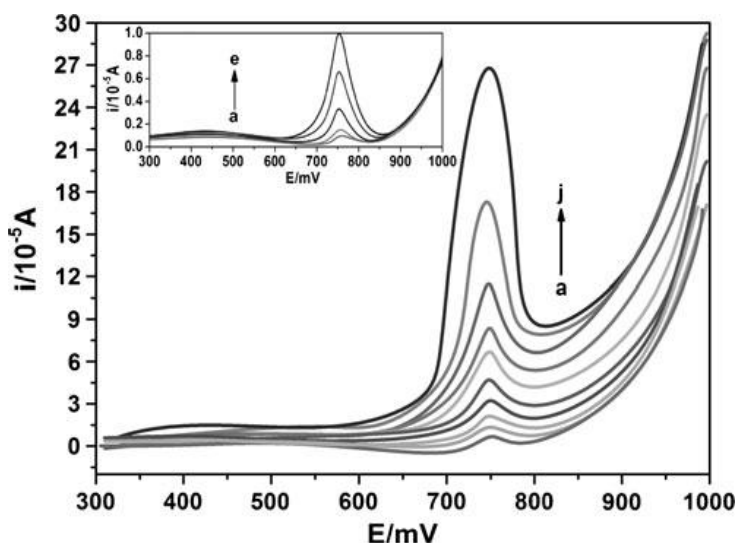


**Figure 4.** DPVs at GO-MWCNT/GCE with different concentrations of L-tyrosine (a to j: 1.0 to 650.0  $\mu\text{M}$ ). Inset: DPVs of L-tyrosine with low concentrations (a to e: 0.05 to 1.0  $\mu\text{M}$ ) (Reproduced with permission from ref. [80]).

Li and co-workers [80] fabricated a simple electrochemical sensor based on GO-CNT modified GCE for the sensitive determination of L-tyrosine. The GO-CNT hybrid based tyrosine sensor exhibited wide linear range, low detection limit, excellent selectivity. The excellent analytical parameters achieved at the hybrid modified electrode and appreciable practicality of the proposed sensor proved the efficiency of the hybrid towards the determination of L-tyrosine (Fig. 4).

Luo et al. [79] constructed a simple, sensitive, and selective voltammetric sensor for the efficient determination of carbendazim by DPV at GO-CNT hybrid film modified GCE. The CV and DPV results of the hybrid film modified electrode towards the electrocatalysis of carbendazim proved the enhanced catalytic ability of the hybrid than that of pure GO or CNTs. The effective area of the GO-CNT hybrid, anodic transfer coefficient, and apparent diffusion coefficient were calculated and it was found that the electrocatalytic process on the modified electrode was diffusion controlled irreversible process. The GO-CNT modified GCE based carbendazim sensor owned excellent

analytical parameters with the high linear range of 10 nM to 4  $\mu$ M and low detection limit of 5 nM. Moreover, the practicality of the fabricated sensor was demonstrated in soil and tap water which showed acceptable recoveries.

#### 4.5 Biosensors

Zhang and co-workers [74] constructed GO-MWCNT hybrid nanocomposite based electrochemical platform for the direct electrochemistry of HRP. HRP immobilization has been achieved by the electrostatic interaction between negatively charged GO-MWCNT hybrids with positively charged HRP aqueous solution of pH 5.0. The modified electrode exhibited excellent electrocatalytic activity towards the reduction of  $\text{H}_2\text{O}_2$  with broad linear range of 3.5 to 293  $\mu$ M, low detection limit of 1.17  $\mu$ M and high sensitivity of 563.7  $\text{mA cm}^{-2} \text{M}^{-1}$ . In addition, the HRP/GO-MWCNT modified electrode exhibited good electrocatalytic ability towards the reduction of nitrite with linear range of 36–316 mM, detection limit of 12 mM and sensitivity of 0.6  $\text{mA cm}^{-2} \text{M}^{-1}$ . Therefore, the GO-MWCNT hybrid nanomaterials could be a good sensing platform for the immobilization of the redox proteins and enzymes.

Our research group [108] demonstrated the use of GO-CNT hybrid material for the preparation of novel nanocomposite with Iron Phthalocyanine (FePc) and employed it for the electrochemical determination of hydrazine. We performed amperometric i-t experiments, for every addition, a prompt defined amperometric responses were observed in the linear hydrazine concentrations between  $5 \times 10^{-7}$ – $8.35 \times 10^{-5}$  M. The outstanding electrocatalytic ability of the GO-CNT-FePc composite material compared with bare GCE and other modified electrodes could be possibly due to the synergy between GO dispersed CNT and FePc, because either pure CNT or FePc does not exhibited good performance.

## 5. APPLICATIONS OF THE GRAPHENE-CNT HYBRID

Similar like GO-CNT hybrid, its reduced form graphene-CNT hybrid material also applied for the numerous applications including electronics [109-113], supercapacitors [84-86, 98 -99,101, 114-119], Li-ion batteries [93-94, 120-124], dye sensitized solar cells [66, 90] sensors [103, 105, 108, 125-127] and biosensors [64, 96, 128].

### 5.1 Electronics

Graphene-CNT or RGO-CNT hybrid materials and their transparent thin films are shown profound impact in electronics applications and transparent conductors [109-113]. For Instance, Deng et al. [109] prepared graphene-CNT hybrid of excellent field emission characteristics by using radio frequency hydrogen plasma sputtering deposition. The hybrid exhibited excellent field emission properties superior than pristine CNT arrays, with low turn-on electric field of 0.98 V/ $\mu$ m, threshold field of 1.51 V/ $\mu$ m, low work function of 4.67 eV, large field enhancement factor of 3980 and good

stability behavior. The results suggested that the prepared graphene-CNT hybrid could be a promising material for the development of high performance field emitters.

Nguyen and co-workers reported a facile technique for the preparation of controlled growth of graphene-CNT hybrid material for the flexible and transparent conductors and electron field emitters. Compared with pristine graphene film, graphene-CNT hybrid film showed significantly improved sheet resistance of  $420 \text{ k}\Omega \text{ sq}^{-1}$  with an optical transmittance of 72.9%. Owing to the low contact resistance of the hybrid films, they were established as an efficient electron field emitters of low turn-on ( $2.9 \text{ V } \mu\text{m}^{-1}$ ) and threshold electric fields ( $3.3 \text{ V } \mu\text{m}^{-1}$ ). The developed graphene-CNT films hold great promise in the fields of flexible optoelectronics, transparent conductors and electron field emitters.

### 5.2 Supercapacitors

Numerous efforts were taken to exploit the highly conducting graphene-CNT hybrid material for the applications as supercapacitors [84-86, 98 -99,101, 114-119]. Cheng and co-workers [84] fabricated a graphene-CNT composite film based high energy density supercapacitors with specific capacitance of  $290.4 \text{ F g}^{-1}$  (aqueous electrolytes) and  $201.0 \text{ F g}^{-1}$  (organic electrolytes) for a single electrode using a more practical two-electrode testing system. The authors obtained energy density of  $62.8 \text{ Wh kg}^{-1}$  and a power density of  $58.5 \text{ kW kg}^{-1}$ , which were 23% and 31% higher than using a pristine graphene electrode in an organic electrolyte, respectively. Moreover, the fabricated graphene-CNT hybrid based supercapacitors exhibited excellent cyclic stability. The outstanding performance of the hybrid based supercapacitors in terms of high energy and power performances, made the hybrid as a promising candidate for its usage in hybrid vehicles and electrical vehicles.

Lin and co-workers [114] fabricated a microsupercapacitors based on graphene-CNT carpets with seamlessly patterned CNTs grown from the graphene with high electrochemical performance. The fabricated microdevices exhibited much higher energy capacity than the commercial aluminum electrolytic capacitors and having comparable alternating current line filtering applications. The fabricated devices delivered maximum power density of  $115 \text{ W/cm}^3$  in aqueous electrolyte and achieved specific capacitances up to  $2.16 \text{ mF/cm}^2$  in (aqueous electrolytes)  $3.93 \text{ mF/cm}^2$  (ionic liquids) comparable to other best supercapacitors. Therefore, the authors strongly believed that the exceptional characters owned by the hybrid could satisfy the need and demands of the future microscale energy storage devices.

### 5.3. Dye sensitized solar cells

Yen and co-workers [66] synthesized graphene-MWCNT hybrid from graphene and acid treated MWCNTs via solution based method and employed it as photoanodes for the DSSCs [Fig. 5]. Under light illumination, DSSC fabricated using the hybrid composite as photoanode showed significantly improvement performance compared with that of pristine  $\text{TiO}_2$  electrode and provide 31 % increase in photocurrent and 35 % improvement in the conversion efficiency. The high specific surface area and improved electrical paths were the possible reasons for the high cell performance of

hybrid DSSC devices. Moreover, the hybrid increases the adsorption of dye, enhances the electrical conductive path and decreases the charge recombination process and thus provides enormous potential for the further DSSC applications.

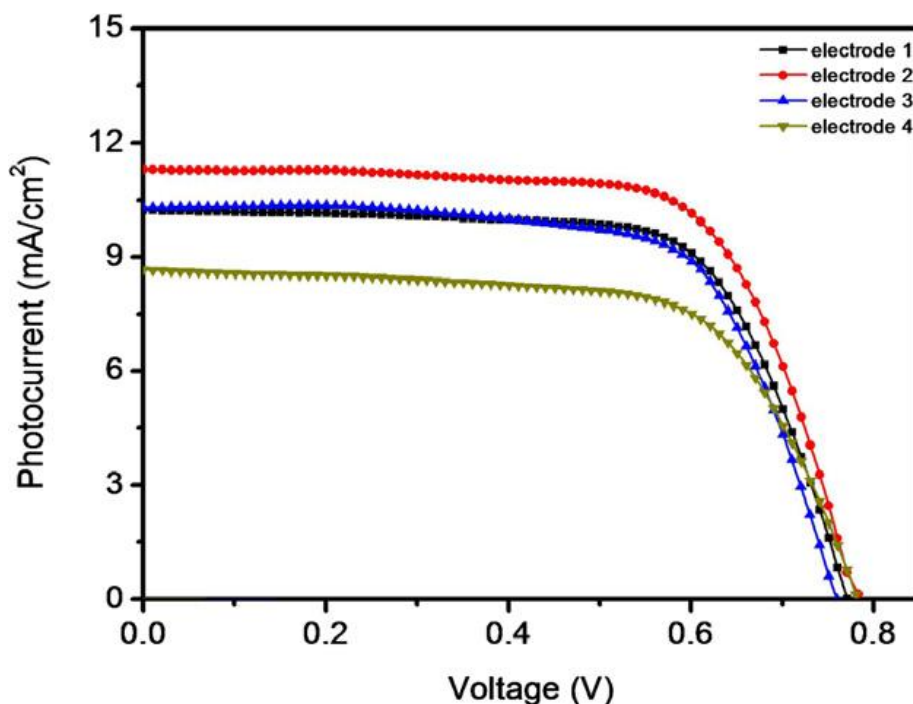


**Figure 5.** Photocurrent density–voltage characteristics of the different electrodes. Here, electrode 1, electrode 2, electrode 3 and electrode 4 represent pristine CNT, graphene-MWCNT hybrid, pristine graphene and pristine TiO<sub>2</sub> respectively (Reproduced with permission from ref. [66]).

#### 5.4 Sensors

Our research group reported a highly sensitive amperometric sensor for the determination of carbamazepine (CBZ) at the reduced graphene oxide RGO-SWCNT hybrid film modified GCE [108]. Compared with pristine SWCNT modified electrode, RGO-SWCNT composite film modified electrode exhibited 3.2 fold enhancements for the electro-oxidation of CBZ. The constructed amperometric sensor exhibited very low detection limit of 29 nM and has a sensitivity of 5.1076  $\mu\text{A } \mu\text{M}^{-1}\text{cm}^{-2}$  with the linear range of 50 nM to 3  $\mu\text{M}$ . The real sample studies performed in the Tegratol tablets revealed the practical application of the proposed sensor. Woo et al. [105] prepared graphene–MWCNT hybrid composite modified electrode and employed it for the electrochemical sensing of H<sub>2</sub>O<sub>2</sub>. The CV results graphene-MWCNT modified electrode (Fig. 6A) showed better electrocatalytic performance than that of either pristine graphene or MWCNT, attributed to the high density of defective sites and high surface area on the graphene–carbon nanotubes composite. Moreover, The hybrid based modified electrode exhibited good performance towards the amperometric determination of H<sub>2</sub>O<sub>2</sub> with detection limit of  $9.4 \times 10^{-6} \text{ mol L}^{-1}$  and good linear dependence on H<sub>2</sub>O<sub>2</sub> concentration in the range of  $2 \times 10^{-5}$  to  $2.1 \times 10^{-3} \text{ mol L}^{-1}$  (Fig. 6B). This study provides a new kind of composite modified electrode for electrochemical sensors. The synergistic effect between graphene sheets and

CNTs might be the reason for the better electrocatalytic performance of the hybrid and eventually the prepared composite will find promising applications in the fabrication of various devices.

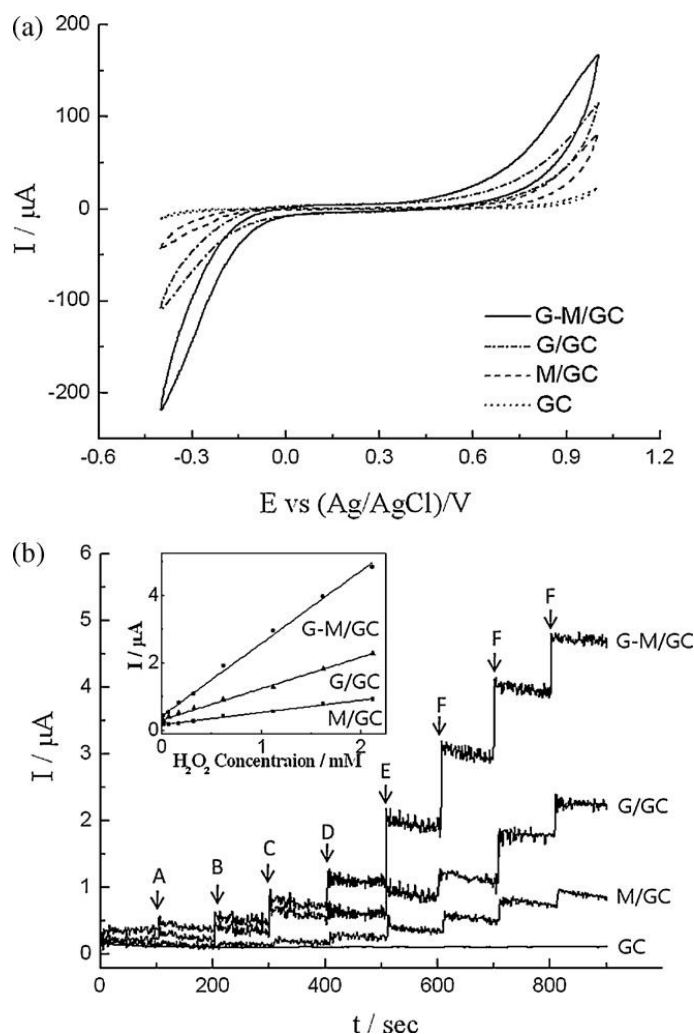


**Figure 6.** (a) CVs of GC (dotted line), M(MWCNT)/GC (dashed line), G(graphene)/GC (dash-dotted line), and G-M(graphene-MWCNT hybrid)/GC (solid line) electrodes towards 4 mM  $\text{H}_2\text{O}_2$  in PBS at the scan rate of  $50 \text{ mV s}^{-1}$ . (b) Amperometric  $i$ - $t$  curves at GC, M/GC, G/GC, and G-M/GC electrode with additions of  $\text{H}_2\text{O}_2$  in PBS. Applied potential:  $-0.4 \text{ V}$ , concentration of  $\text{H}_2\text{O}_2$ : (A)  $2.0 \times 10^{-5}$ , (B)  $5.0 \times 10^{-5}$ , (C)  $1.0 \times 10^{-4}$ , (D)  $1.5 \times 10^{-4}$ , (E)  $3.0 \times 10^{-4}$ , and (F)  $5.0 \times 10^{-4} \text{ mol L}^{-1}$ . Inset shows their respective calibration curves (Reproduced with permission from ref. [105]).

Chen and co-workers [126] fabricated a graphene-SWCNT hybrid film modified electrode and employed it for the electrochemical determination of acetaminophen by differential pulse voltammetry (DPV). The proposed graphene-SWCNT modified electrode based electrochemical sensor exhibited excellent analytical performance towards sensing of acetaminophen with low detection limit of 38 nM and wide sensor working linear range of 0.05–64.5  $\mu\text{M}$ . Moreover, the proposed sensor exhibited good selectivity and stability. The excellent performances of the hybrid sensor were mainly ascribed to the large surface area and multi-modal pore structure of the 3D network of the graphene-SWCNT.

## 5.5 Biosensors

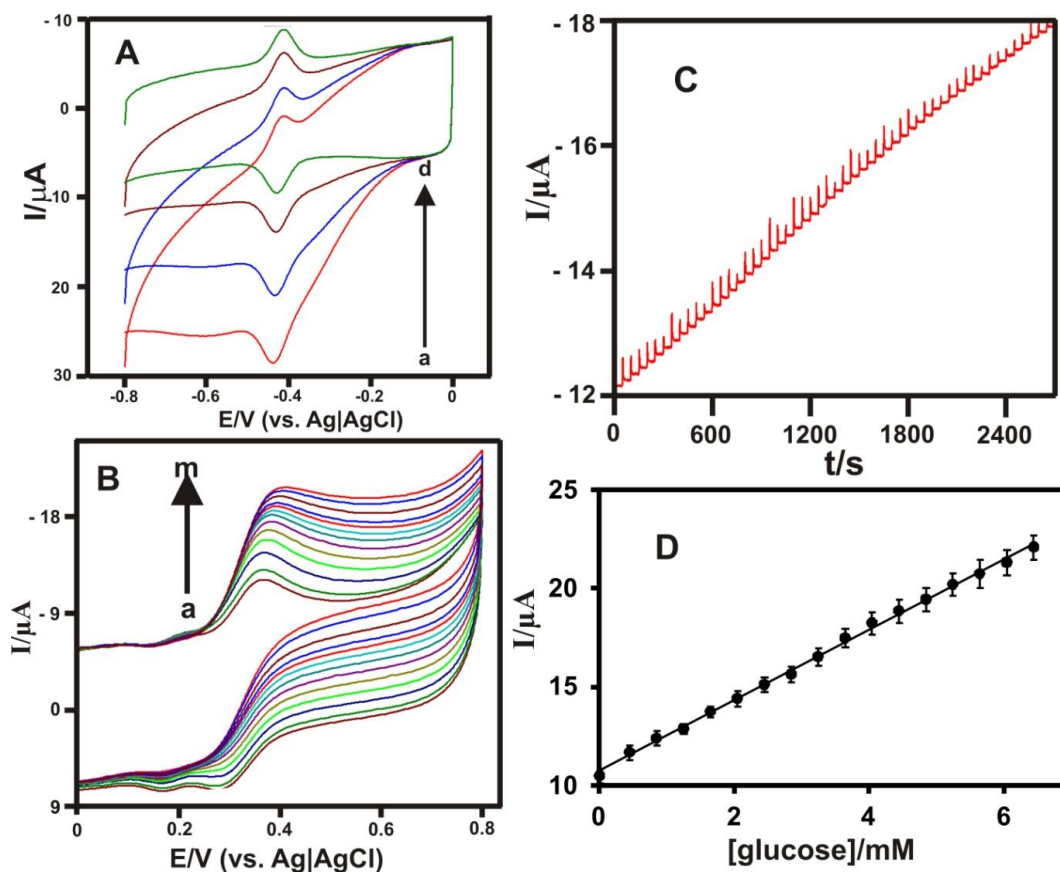


**Figure 7.** (A) CVs of RGO-MWCNT/GOx/Nf/GCE in oxygenated PBS without glucose (a) with the additions of glucose 0.1 (b), 1 (b) and 2 mM (c). (B) CVs of RGO-MWCNT/GOx/Nf/GCE in PBS (pH 7) containing 0.5mM FMCA without glucose (a) and with each additions of 0.4 mM glucose. (b to m, from 0.4 mM to 4.8 mM). C) Amperometric i-t obtained at RGO-MWCNT/GOx/Nf modified rotating disc electrode upon successive additions of 50  $\mu\text{M}$  glucose into PBS (pH 7) containing 0.5 mM FMCA. Rotation rate: 1500 rpm;  $E_{\text{app}} = +0.35\text{V}$ . B) Calibration plot of [glucose] vs. peak current.  $I_p/\mu\text{A} = 10.36 (\pm) \mu\text{A} + 1.908(\pm) [\text{glucose}]/\mu\text{A mM}^{-1}$  (Reproduced with permission from [64]).

Our research group prepared RGO-CNT hybrid for the enhanced direct electrochemistry of GOx and employed the modified electrode towards the amperometric determination of glucose [64]. The low peak to peak separation ( $\Delta E_p$ ) of 26 mV and high electron transfer rate constant value ( $3.02 \text{ s}^{-1}$ ) were proved that the electron transfer at the hybrid modified film was significantly higher than either RGO or MWCNT alone. We demonstrated the electrochemical determination of glucose via both reductive detection of oxygen consumption (first generation glucose biosensor) and redox mediator ferrocene mono carboxylic acid (second generation glucose biosensor). In both the cases, the hybrid composite have owned excellent ability to determine the glucose. The amperometric i-t experiments displayed well defined amperometric responses the each addition of glucose and the amperometric current responses were increased linearly with the glucose concentrations of 10  $\mu\text{M}$  to 6.5 mM (Fig. 7). The excellent analytical parameters of high sensitivity of  $7.95 \mu\text{A mM}^{-1} \text{ cm}^{-2}$  and very low detection

limit of 4.7  $\mu\text{M}$  showed the efficiency of the RGO-MWCNT hybrid towards the efficient determination of glucose.

Dong et al. [96] prepared graphene–CNT hybrid foam by two-step CVD method under atmospheric pressure and utilized it for the immobilization of the enzyme horseradish peroxidase (HRP). Moreover the authors demonstrated efficient electrochemical sensors for the determination of dopamine and  $\text{H}_2\text{O}_2$  using the graphene-CNT and graphene-CNT/HRP/Nf hybrid films modified electrodes respectively. The hybrid film modified electrode exhibited good electrocatalytic ability towards the determination of dopamine with excellent analytical parameters such as high sensitivity of  $470.7 \text{ mA M}^{-1} \text{ cm}^{-2}$  and low detection limit of 20 nM. Similarly the graphene-CNT/HRP/Nf modified electrode showed excellent electrocatalytic activity for the determination of  $\text{H}_2\text{O}_2$  with high sensitivity of  $137.9 \text{ mA M}^{-1} \text{ cm}^{-2}$ , low detection limit of 1  $\mu\text{M}$  and wide sensor working range of of 10  $\mu\text{M}^{-1} \text{ mM}$ . The efficient electrocatalytic ability of the hybrid could be ascribed due to the large active surface area provided by the integrated 3D network of graphene foam and CNT nanomesh, in addition with high conductivity and fast electron transfer of the integrated hybrid.

## 6. CONCLUSIONS

Thus, the GO/graphene-CNT hybrid nanomaterials were special kind of hybrid materials with superior performance than the pristine CNT or GO/graphene materials. The various preparation methodologies for the GO/graphene-CNT hybrid materials were presented in detail. Moreover, we discussed the numerous characterization techniques and various applications of the hybrid materials in diverse field of research such as electronics, supercapacitors, batteries DSSCs, sensors and biosensors. In most of the cases, the hybrid showed superior performance than the pristine GO/graphene or CNT materials owing to the special structural arrangement with 3D hierarchical network. This arrangement makes it possible to acquire the maximum edge density per unit nominal area than the pristine GO/graphene or CNT. Still much room is available for the new ideas in the preparation and processing of GO/graphene-CNT hybrid materials.

## ACKNOWLEDGEMENT

This work was supported by the National Science Council and the Ministry of Education of Taiwan (Republic of China).

## References

1. K.S. Novoselov, A.K. Geim, S.V. Morozov, D. Jiang, Y. Zhang, S.V. Dubonos, I.V. Grigorieva, A.A. Firsov, *Science*, 306 (2004) 666.
2. S.W. Ting, A.P. Periasamy, S.-M. Chen, R. Saraswathi, *Int. J. Electrochem. Sci.*, 6 (2011) 4438.
3. K.S. Novoselov, V.I. Falko, L. Colombo, P.R. Gellert, M.G. Schwab, K. Kim, *nature*, 490 (2012) 192.
4. C.N.R. Rao, A.K. Sood, R. Voggu, K. S. Subrahmanyam, *J. Phys. Chem. Lett.*, 1 (2010) 572.
5. B. Devadas, M. Rajkumar, S.-M. Chen, R. Saraswathi, *Int. J. Electrochem. Sci.*, 7(2012) 3339.

6. A.K. Geim, K.S. Novoselov, *Nat.Mater.* 6 (2007) 183.
7. A.K. Geim, *Science*, 324 (2009) 1530.
8. L. Tang, Y. Wang, Y. Li, H. Feng, J. Lu, J. Li, *Adv. Funct. Mater.*, 19 (2009) 2782.
9. J.W. Suk, R.D. Piner, J. An, R.S. Ruoff, *ACS Nano*, 4 (2010) 6567.
10. X.-M. Chen, G.-H. Wu, Y.-Q. Jiang, Y. Wang, X. Chen, *Analyst*, 136 (2011) 4631.
11. P. Avouris, F. Xia, *MRS Bull.*, 37 (2012) 1225.
12. N. Zhang, Y. Zhang, Y.-J. Xu, *Nanoscale*, 4 (2012) 5792.
13. T.-H. Tsai, S.-C. Chiou, S.-M. Chen, *Int. J. Electrochem. Sci.*, 6 (2011) 3333.
14. K. Zhang, L.L. Zhang, X.S. Zhao, J. Wu, *Chem. Mater.* 22 (2010) 1392.
15. K. Yang, L. Feng, X. Shi, Z. Liu, *Chem. Soc. Rev.*, 2013, 42, 530.
16. V. Mani, A.P. Periasamy, S.-M. Chen, *Electrochem. Commun.* 17 (2012) 75.
17. S.W. Ting, A.P. Periasamy, S.-M. Chen, R. Saraswathi, *Int. J. Electrochem. Sci.*, 6 (2011) 4438.
18. D. Chen, L. Tang, J. Li, *Chem. Soc. Rev.*, 2010, 39, 3157.
19. C. Mattevi, H. Kim, M. Chhowall, *J. Mater. Chem.*, 21 (2011) 3324.
20. D. Wei, B. Wu, Y. Guo, G. Yu, Y. Liu, *Acc. Chem. Res.*, 46 (2013) 106.
21. T. Peng, H. Lv, D. He, M. Pan, S. Mu, *Sci Rep.* 3 (2013) 1148.
22. S.W. Poon, W. Chen, E.S. Tok, A.T. Wee, *Appl. Phys. Lett.*, 92 (2008) 104102.
23. A.D. Lueking, L. Pan, D.L. Narayanan, C.E.B. Clifford, *J. Phys. Chem. B* 109 (2005) 12710.
24. E.H.L. Falcao, R.G. Blair, J.J. Mack, L.M. Viculis, C-W. Kwon, M. Bendikov, R.B. Kaner, B.S. Dunn, F.Wudl, *Carbon*, 45 (2007) 1364.
25. R. Hao, W. Qian, L. Zhang, Y. Hou, *Chem. Commun.*, 0 (2008) 6576.
26. H. Huang, Y. Xia, X. Tao, J. Du, J. Fang, Y. Gan, W. Zhang, *J. Mater. Chem.*, 22 (2012) 10452.
27. R.P.B.D. Santos, E. Perim, P.A.S. Autreto, G. Brunetto, D.S. Galvao, *Nanotechnology*, 23 (2012) 465702.
28. N.L. Rangel, J.C. Sotelo, J.M. Seminario, *J. Chem. Phys.* 131 (2009) 031105.
29. S. Stankovich, D.A. Dikin, R.D. Piner, K.A. Kohlhaas, A. Kleinhammes, Y. Jia, Y. Wu, S.T. Nguyen, R.S. Ruoff, *Carbon* 45 (2007) 1558.
30. S. Park, J. An, J.R. Potts, A. Velamakanni, S. Murali, R.S. Ruoff, *carbon*, 49 (2011) 3019.
31. B.C. Brodie, *Philos. Trans. R. Soc. London*, 149 (1859) 249.
32. L. Staudenmaier, *Ber. Dtsch. Chem. Ges.*, 31 (1898) 1481.
33. W.S. Hummers, R.E. Offeman, *J. Am. Chem. Soc.*, 80 (1958) 1339.
34. S. Park, R.S. Ruoff, *Nat. Nanotechnol.*, 4 (2009) 217.
35. Y. Zhu, S. Murali, M.D. Stoller, A. Velamakanni, R.D. Piner, R.S. Ruoff, *Carbon*, 48 (2010) 2106.
36. H.A. Becerril, J. Mao, Z. Liu, R.M. Stoltenberg, Z. Bao, Y. Chen, *ACS Nano*, 2 (2008) 463.
37. T.-Y. Zhang, D. Zhang, *Bull. Mater. Sci.*, 34 (2011) 25.
38. H.-J. Shin, K.K. Kim, A. Benayad, S.-M. Yoon, H.K. Park, I.-S. Jung, M.H. Jin, H.-K. Jeong, J.M. Kim, J.-Y. Choi, Y.H. Lee, *Adv. Funct. Mater.*, 19 (2009) 1987.
39. G. Wang, J. Yang, J. Park, X. Gou, B. Wang, H. Liu, J. Yao, *J. Phys. Chem., C*, 112 (2008) 8192.
40. J. Zhang, H. Yang, G. Shen, P. Cheng, J. Zhang, S. Guo, *Chem. Commun.*, 46 (2010) 1112.
41. D.R. Dreyer, S. Murali, Y. Zhu, R.S. Ruoff, C.W. Bielawski, *J. Mater. Chem.*, 21 (2011) 3443.
42. X. Fan, W. Peng, Y. Li, X. Li, S. Wang, G. Zhang and F. Zhang, *Adv. Mater.*, 20 (2008) 4490.
43. T. Zhou, F. Chen, K. Liu, H. Deng, Q. Zhang, J. Feng, Q. Fu, *Nanotechnology*, 22 (2011) 045704.
44. C. Zhu, S. Guo, Y. Fang, S. Dong, *ACS Nano*, 4 (2010) 2429.
45. H.C. Schniepp, J.-L. Li, M.J. McAllister, H. Sai, M.H.-Alonso, D.H. Adamson, R.K. Prudhomme, R. Car, D.A. Saville, I.A. Aksay, *J. Phys. Chem. B*, 110 (2006) 8535.
46. M. Zhou, Y. Wang, Y. Zhai, J. Zhai, W. Ren, F. Wang, S. Dong, *Chem. Eur. J.*, 15 (2009) 6116.
47. H.-L. Guo, X.-F. Wang, Q.-Y. Qian, F.-B. Wang, X.-H. Xia, *ACS nano*, 3 (2009) 2653.
48. W. Choi, I. Lahiri, R. Seelaboyina, Y.S. Kang, *Crit. Rev. Solid State Mater. Sci.*, 35 (2010) 52.
49. D.R. Dreyer, S. Park, C.W. Bielawski, R.S. Ruoff, *Chem. Soc. Rev.*, 39 (2010) 228.
50. L. Qiu, X. Yang, X. Gou, W. Yang, Z.F. Ma, G.G. Wallace, D. Li, *Chem. Eur. J.*, 16 (2010) 10653.

51. F. Kim, L.J. Cote, J. Huang, *Adv. Mater.*, 22 (2010) 1954.
52. T. Szabo, O. Berkesi, P. Forgo, K. Josepovits, Y. Sanakis, D. Petridis, I. Dekany, *Chem. Mater.*, 18 (2006) 2740.
53. Z. Liu, J. T. Robinson, X. Sun, H. Dai, *J. Am. Chem. Soc.*, 130 (2008) 10876.
54. H. Yang, F. Li, C. Shan, D. Han, Q. Zhang, L. Niu, A. Ivaska, *J. Mater. Chem.*, 19 (2009) 4632.
55. Y.X. Xu, H. Bai, G.W. Lu, C. Li, G.Q. Shi, *J. Am. Chem. Soc.*, 130 (2008) 5856.
56. S. Iijima, *Nature*, 354 (1991) 56.
57. S. Niogi, M.A. Hamon, H.Hu, B.Zhao, P. Bhowmik, R. Sen, M.E. Itkis, R.C. Haddon, *Acc. Chem. Res.*, 35 (2002) 1105.
58. K.-C. Lin, C.-P. Hong, S.-M. Chen, *Int. J. Electrochem. Sci.*, 7(2012) 11426.
59. B. Unnikrishnan, Y. Umasankar, S.-M. Chen, C.-C. Ti, *Int. J. Electrochem. Sci.*, 7 (2012) 3047.
60. R. Martel, T. Schmidt, H.R. Shea, T. Hertel, P. Avouris, *Appl. Phys. Lett.*, 73 (1998) 2447.
61. Y. Kang, T.A. Taton, *J. Am. Chem. Soc.*, 125 (2003) 5650.
62. R.T. Kachoosangi, M.M. Musameh, I.A.-Yousef, J.M. Yousef, S.M. Kanan, L. Xiao, S.G. Davies, A. Russell, R.G. Compton, *Anal. Chem.*, 81 (2009) 435.
63. J.L. Bahr, J. Yang, D.V. Kosynkin, M.J. Bronikowski, R.E. Smalley, J.M. Tour, *J. Am. Chem. Soc.*, 123 (2001) 6536.
64. V. Mani, B. Devadas, S.-M. Chen, *Biosens.Bioelectron.* 41(2013) 309.
65. B. Devadas, V. Mani, S.-M. Chen, *Int. J. Electrochem. Sci.*, 7 (2012) 8064.
66. M.-Y. Yen, M-C. Hsiao, S.-H. Liao, P.-I. Liu, H.-M. Tsai, C.-C. M. Ma, N.-W. Pu, M.-D. Ger, *Carbon*, 49 (2011) 3597.
67. X. Dong, B. Li, A. Wei, X. Cao, M.B.C.-Park, H. Zhang, L.-J. Li, W. Huang, P. Chen, *Carbon*, 49 (2011) 2944.
68. P. Han, Y. Yue, Z. Liu, W. Xu, L. Zhang, H. Xu, S. Dong, G. Cui, *Energy Environ. Sci.*, 4 (2011) 4710.
69. C. Zhang, L. Ren, X. Wang, T. Liu, *J. Phys. Chem. C*, 114 (2010) 11435.
70. B.R. Stoner, J.T. Glass, *Diamond Relat. Mater.*, 23 (2012) 130.
71. L. Buglione, M. Pumera, *Electrochem. Commun.* 17 (2012) 45.
72. L. Tian, M.J. Meziani, F. Lu, C.Y. Kong, L. Cao, T.J. Thorne, Y.-P. Sun, *ACS Appl. Mater. Interfaces*, 2 (2010) 3217.
73. S.H.Aboutalebi, A.T. Chidembo, M. Salari, K. Konstantinov, D. Wexler, H.K. Liu, S.X. Dou, *Energy Environ. Sci.*, 4 (2011) 1855.
74. Q. Zhang, S. Yang, J. Zhang, L. Zhang, P. Kang, J. Li, J. Xu, H. Zhou, X.-Mi. Song, *Nanotechnology*, 22 (2011) 494010.
75. X. Dong, G. Xing, M.B.C.-Park, W. Shi, N. Xiao, J. Wang, Q. Yan, T.C. Sum, W. Huang, P. Chen, *Carbon*, 49 (2011) 5071.
76. V.C. Tung, J. Kim, J. Huang, *Adv. Energy Mater.*, 2 (2012) 299.
77. J.-J. Shao, W. Lv, Q. Guo, C. Zhang, Q. Xu, Q.-H. Yang, F. Kang, *Chem. Commun.*, 48 (2012) 3706.
78. B. You, N. Li, H. Zhu, X. Zhu, J. Yang, *ChemSusChem*, 6 (2013), 474.
79. S. Luo, Y. Wu, H. Gou, *Ionics*, 19 (2013) 673.
80. J. Li, D. Kuang, Y. Feng, F. Zhang, Z. Xu, M. Liu, D. Wang, *Microchim Acta*, 180 (2013) 49.
81. K. Sablok, V. Bhalla, P. Sharma, R. Kaushal, S. Chaudhary, C.R. Suri, *J. Hazard. Mater.*, 248 (2013) 322.
82. Q. Zheng, B. Zhang, X. Lin, X. Shen, N. Yousefi, Z.-D. Huang, Z. Li, J.-K. Kim, *J. Mater. Chem.*, 22 (2012) 25072.
83. Y.-K. Kim, D.-H. Min, *Carbon*, 48 (2010) 4283.
84. Q. Cheng, J. Tang, J. Ma, H. Zhang, N. Shinya, L.-C. Qinc, *Phys. Chem. Chem. Phys.*, 13 (2011) 17615.

85. S.-Y. Yang, K.-H. Chang, H.-W. Tien, Y.-F. Lee, S.-M. Li, Y.-S. Wang, J.-Y. Wang, C.-C.M. Ma, C.-C. Hu, *J. Mater. Chem.*, 21 (2011) 2374.
86. J. Lu, H. Dou, B. Gao, C. Yuan, S. Yang, L. Hao, L. Shen, X. Zhang, *Electrochim. Acta*, 56 (2011) 5115.
87. X.Y. Wang, Y. Wu, Y. Huang, F. Zhang, X. Yang, Y. Ma, Y. Chen, *J. Phys. Chem. C*, 115 (2011) 23192.
88. D. Zhang, T. Yan, L. Shi, Z. Peng, X. Wen, J. Zhang, *J. Mater. Chem.*, 22 (2012) 14696.
89. J. Chen, X. Zheng, F. Miao, J. Zhang, X. Cui, W. Zheng, *J Appl Electrochem* 42 (2012) 875.
90. L.-H. Chang, C.-K. Hsieh, M.-C. Hsiao, J.-C. Chiang, P.-I. Liu, K.-K. Ho, C.-C.M. Ma, M.-Y. Yen, M.-C. Tsai, C.-H. Tsai, *J. Power Sources*, 222 (2013) 518.
91. Z. Sui, Q. Meng, X. Zhang, R. Ma, B. Cao, *J. Mater. Chem.*, 22 (2012) 8767.
92. Y.-T. Liu, M. Dang, X.-M. Xie, Z.-F. Wang, X.-Y. Ye, *J. Mater. Chem.*, 21 (2011) 18723.
93. S. Li, Y. Luo, W. Lv, W. Yu, S. Wu, P. Hou, Q. Yang, Q. Meng, C. Liu, H.-M. Cheng, *Adv. Energy Mater.*, 1 (2011) 486.
94. S. Chen, P. Chen, Y. Wang, *Nanoscale*, 3 (2011) 4323.
95. U.J. Kim, I.H. Lee, J.J. Bae, S. Lee, G.H. Han, S.J. Chae, F. Günes, J.H. Choi, C.W. Baik, S.I. Kim, J.M. Kim, Y.H. Lee, *Adv. Mater.*, 23 (2011) 3809.
96. X. Dong, Y. Ma, G. Zhu, Y. Huang, J. Wang, M.B.C.-Park, L. Wang, W. Huang, P. Chen, *J. Mater. Chem.*, 22 (2012) 17044.
97. R. Atchudan, J. Joo, A. Pandurangan, *Mater. Res. Bull.*, 48 (2013) 2205.
98. M.-Q. Zhao, Q. Zhang, J.-Q. Huang, G.-L. Tian, T.-C. Chen, W.-Z. Qian, F. Wei, *Carbon*, 54 (2013) 403.
99. Z. Fan, J. Yan, L. Zhi, Q. Zhang, T. Wei, J. Feng, M. Zhang, W. Qian, F. Wei, *Adv. Mater.*, 22 (2010) 3723.
100. D.H. Lee, J.E. Kim, T.H. Han, J.W. Hwang, S. Jeon, S.-Y. Choi, S.H. Hong, W.J. Lee, R.S. Ruoff, S.O. Kim, *Adv. Mater.*, 22 (2010) 1247.
101. Z.-D. Huang, B. Zhang, S.-W. Oh, Q.-B. Zheng, X.-Y. Lin, N. Yousefi, J.-K. Kim, *J. Mater. Chem.*, 22 (2012) 3591.
102. Y.-F. Li, Y.-Z. Liu, Y.-G. Yang, M.-Z. Wang, Y.-F. Wen, *Appl Phys A*, 108 (2012) 701.
103. Z.H. Wang, S.Y. Yao, J.F. Xia, F.F. Zhang, X.M. Guo, Y.Z. Xia, Y.H. Li, *Adv. Mater. Res.*, 531 (2012) 419.
104. S. Sasikaladevi, J. Aravind, V. Eswaraiah, S. Ramaprabhu *J. Mater. Chem.*, 21 (2011) 15179.
105. S. Woo, Y.-R. Kim, T.D. Chung, Y. Piao, H. Kim, *Electrochim. Acta*, 59 (2012) 509.
106. J. Kim, V.C. Tung, J. Huang, *Adv. Energy Mater.* 1 (2011) 1052.
107. V.C. Tung, J. Kim, J. Huang, *Adv. Energy Mater.*, 2 (2012) 299.
108. V. Mani, A.T.E. Vilian, S.-M. Chen, *Int. J. Electrochem. Sci.*, 7 (2012) 12774.
109. J.-H. Deng, R.-T. Zheng, Y.-M. Yang, Y. Zhao, G.-A. Cheng, *Carbon*, 50 (2012) 4732.
110. J.-H. Deng, R.-T. Zheng, Y. Zhao, G.-A. Cheng, *ACS Nano*, 6 (2012) 3727.
111. D.D. Nguyen, N.-H. Tai, S.-Y. Chen, Y.-L. Chueh, *Nanoscale*, 4 (2012) 632.
112. J.-H. Huang, J.-H. Fang, C.-C. Liu, C.-W. Chu, *ACS Nano*, 5 (2011) 6262.
113. T.-K. Hong, D.W. Lee, H.J. Choi, H.S. Shin, B.-S. Kim, 4 (2010) 3861.
114. J. Lin, C. Zhang, Z. Yan, Y. Zhu, Z. Peng, R.H. Hauge, D. Natelson, J.M. Tour, *Nano Lett.* 13 (2013) 72.
115. D. Yu, L. Dai, *J. Phys. Chem. Lett.*, 1 (2010) 467.
116. Y. Wu, T. Zhang, F. Zhang, Y. Wang, Y. Ma, Y. Huang, Y. Liu, Y. Chen, *Nano Energy*, 1 (2012) 820.
117. Y.-S. Kim, K. Kumar, F.T. Fisher, E.-H. Yang, *Nanotechnology*, 23 (2012) 015301.
118. Y.-F. Li, Y.-Z. Liu, Y.-G. Yang, M.-Z. Wang, Y.-F. Wen, *Appl. Phys. A* 108 (2012) 701.
119. P. Tamailarasan, S. Ramaprabhu, *J. Phys. Chem. C*, 116 (2012) 14179.
120. B.P. Vinayan, R. Nagar, V. Raman, N. Rajalakshmi, K.S. Dhathathreyan, S. Ramaprabhu, *J. Mater. Chem.*, 22 (2012) 9949.

- 121.S.-D. Seo, I.-S. Hwang, S.-H. Lee, H.-W. Shim, D.-W. Kim, *Ceram.Int.*, 38 (2012) 3017.
- 122.S. Chen, W. Yeoh, Q. Liu, G. Wang, *Carbon*, 50 (2012) 4557.
- 123.Y. Hu, X. Li, J. Wang, R. Li, X. Sun, *J. Power Sources*, 237 (2013) 41.
- 124.M.-Q. Zhao, X.-F. Liu, Q. Zhang, G.-L. Tian, J.-Q. Huang, W. Zhu, F. Wei, *ACS Nano*, 6 (2012) 10759.
- 125.B. Unnikrishnan, V. Mani, S.-M. Chen, *Sens. Actuators, B*, 173 (2012) 274.
- 126.X. Chen, J. Zhu, Q. Xi, W. Yang, *Sens. Actuators, B*, 161 (2012) 648.
- 127.F. Hu, S. Chen, C. Wang, R. Yuan, D. Yuan, C. Wang, *Anal. Chimi. Acta*, 724 (2012) 40.
- 128.J. Chen, X. Zheng, F. Miao, J. Zhang, X. Cui, W. Zheng, *J. Appl. Electrochem.*, 42 (2012) 875.